Confined protein adsorption into nanopore arrays fabricated by colloidal-assisted polymer patterning†

Grazia M. L. Messina, Cristina Satriano* and Giovanni Marletta

Received (in Cambridge, UK) 9th June 2008, Accepted 14th July 2008
First published as an Advance Article on the web 5th September 2008
DOI: 10.1039/b809664c

A combination of plasma surface modification of polymer thin films and colloidal nanosphere lithography was used to fabricate two-dimensional nanopore arrays as protein nanocontainers.

Surface nanostructuring of polymeric thin films in two-dimensional (2D) porous substrates is an intriguing strategy for various applications including microelectronics, sensing, catalysis, optics and biomedical science.[1–3] For instance, ordered pore arrays have been shown to be very promising as nanocontainers and/or nanoreactors of protein/oligopeptide molecules for controlled drug delivery and highly efficient catalysis applications.[4,5] Indeed, several studies indicate that, by properly tuning of the surface free energy (SFE) properties of the adsorbent substrate, the spontaneous adsorption of (bio)molecules may be significantly influenced in terms of coverage, conformation and process kinetics.[6–8] Moreover, SFE structured surfaces with domains at the micrometer and sub-micrometer size may lead to morphological wetting transition and unusual confinement effects.[9–11]

In this paper we combine the surface modification by oxygen plasma treatment of a polyhydroxymethylsiloxane (PHMS) thin film and the colloidal lithography approach to implement the colloidal crystal-assisted capillary-nanofabrication method (CCACN)[3] in order to pattern the SFE properties at the nanometer scale and to fabricate ordered hydrophilic or hydrophobic pore arrays. Such a strategy overcomes the restrictions to few selected substrates, such as Au, Si and mica, which often occur in the approaches based on self assembling processes aimed to obtain chemical structuring and protein immobilization.[12–14]

Scheme 1 shows the three-step procedure to confine the low- and high-SFE domains at the sub-micrometer scale at the surface of polymeric thin films, and thus obtain hydrophilic (HYL-np) or hydrophobic (HYB-np) nanopores. The self-assembly of polystyrene nanoparticles was observed on polymeric surfaces exhibiting two different SFE behaviors. Atomically flat films (root mean squared roughness values of 0.3 ± 0.1 nm) of PHMS (hydrophobic, with water contact angle of 93° ± 2° and a SFE value of 63 ± 3 mJ m^{-2}) and oxygen-plasma modified PHMS (hydrophilic, water contact angle of 0–5° and SFE = 35 ± 5 mJ m^{-2}),[15] were the substrates employed for polystyrene and carboxylated polystyrene nanoparticles, respectively. Some representative patterns are shown in Fig. 1, which evidences the versatility of the method.

In fact, while the pitch of the array strictly depends on the colloidal particle diameter, the depth and rim appearance may be tuned depending on the specific experimental conditions (*e.g.*, polymer concentration, dewetting rate, humidity, *etc.*...). It is of note that the contrast in the phase images displayed in Fig. 1 is related to the fact that the nanopore structuring is not merely topographical but also chemical, in terms of hydrophobic and hydrophilic domains.[16]

As proof of concept of the working capability of the hydrophobic or hydrophilic nanopore arrays as protein nanocontainers, the immobilization of human lactoferrin (Lf, 0.15 μM in Millipore ultrapure water, pH = 4.42 ± 0.01 at 22 °C) by spontaneous adsorption was investigated.

In particular, the adsorption kinetics, the viscoelastic behavior of the adlayer and the surface coverage were studied by quartz crystal microbalance with dissipation monitoring (QCM-D, QSense) and X-ray photoelectron spectroscopy (XPS, Kratos). Moreover, the morphology of substrates and protein adlayers, both on large areas and on the nanopatterned substrates, was studied by atomic force microscopy (AFM, Nanoscope IIIA, Veeco) operating in tapping mode in air.

The QCM-D plots in Fig. 2 show that upon protein adsorption the shifts of dissipation are quite small compared to those of the frequency curves (Fig. 2(a) and (c)). This finding indicates the formation of a rigid protein adlayer and allows to calculate the amount of adsorbed protein according to Sauerbrey approximation ($\Delta m = -C\Delta F$, where

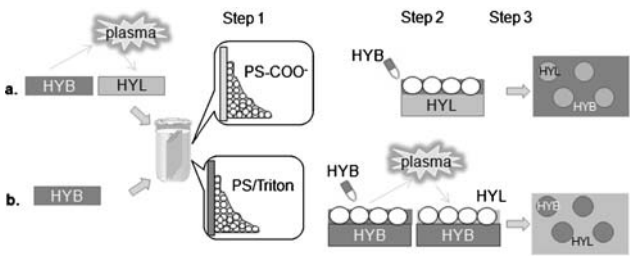

Scheme 1 The three-step method for the fabrication of: (a) HYL-np and (b) HYB-np. (1) Self-assembling driven by solution dewetting of carboxylated polystyrene nanoparticles (PS–COO^-) on hydrophilic (HYL) surfaces (1a), or polystyrene nanoparticles added with a surfactant (PS/Triton) on hydrophobic surfaces (HYB) (1b). (2) A thin film of hydrophobic polymer is added by casting (2a) and, only for HYB-np, converted to a hydrophilic surface by oxygen plasma treatment (2b). Finally, colloidal nanoparticles are removed by sonication (see ESI†).

Laboratory for Molecular Surfaces and Nanotechnologies (LAMSUN) at Department of Chemical Sciences of University of Catania and CSGI, Viale Andrea Doria, 6, 95125 Catania, Italy. E-mail: csatriano@unict.it

† Electronic supplementary information (ESI) available: (1) Full experimental details. (2) XPS figure of C 1s peak for bare and lactoferrin-immobilized surfaces. See DOI: 10.1039/b809664c

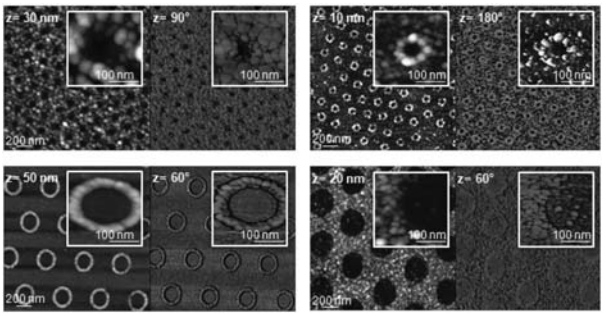

Fig. 1 AFM height (left hand side panel) and phase (right hand side panel) images of nanopore arrays from nanospheres of 209 nm (upper) and 489 nm (lower) of diameter.

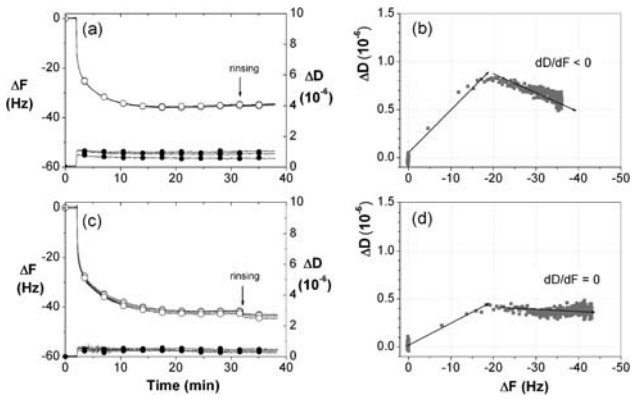

Fig. 2 QCM-D curves of frequency (open symbols, left hand side axis) and dissipation (solid symbols, right hand side axis) for Lf adsorption on (a) hydrophobic and (c) hydrophilic large areas; (b) and (d) are the corresponding *D*–*F* plots. The arrows are drawn to guide the eye.

C is -17.7 ng Hz^{-1} cm^{-2} for the current experimental conditions[17]). The evaluated protein coverages for both HYL and HYB cases correspond to more than an ideal monolayer of closely-packed lactoferrin molecules.[18]‡ Moreover, as well evident by the plots of dissipation *vs.* frequency (*D*–*F* plots), the Lf adlayers exhibit a higher viscoelastic character, *i.e.*, higher curve slope, on the hydrophobic polymer surfaces (Fig. 2(b)) than the hydrophilic ones (Fig. 2(d)). This effect points to the occurrence of different protein aggregation processes at the two surfaces, likely driven by the different surface free energy properties.

In particular, the hydrophobic surfaces likely prompt phenomena, *e.g.*, denaturation, which allow the rigid protein binding to the substrate (the curve slope $\Delta D/\Delta F$ changes from $\sim +0.045 \times 10^{-6}$ Hz^{-1} to a negative value).[19,20] On the other hand, on the hydrophilic surfaces the Lf adsorbed molecules undergo only minor conformational changes, *i.e.*, less or not any denaturation, and substantially keep the same viscoelastic character as that reached at the end of the fast adsorption step ($\Delta D/\Delta F$ changes from $\sim +0.022 \times 10^{-6}$ Hz^{-1} to zero).

According to QCM-D results, the XPS characterization of dried Lf adlayers indicates comparable protein coverage but different average bonding orientation at the protein–polymer interface for hydrophobic and hydrophilic substrates. The similar atomic content of nitrogen, which is the protein-related signal, is about 3–4% for both types of substrates.

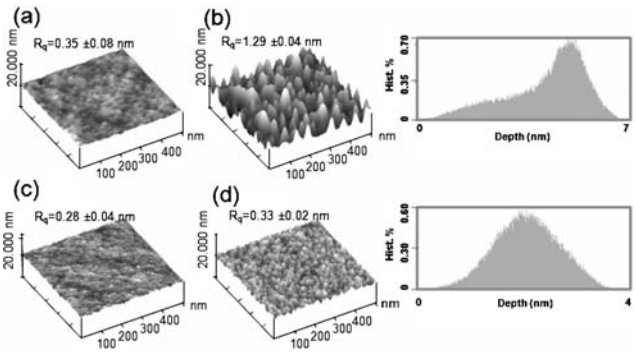

Fig. 3 AFM height images and calculated root mean squared roughness (R_q) of: (a) bare hydrophobic; (b) Lf adsorbed on hydrophobic surface; (c) bare hydrophilic; (d) Lf adsorbed on hydrophilic surface. The histograms contain the grain size analysis results for images (b) and (d).

Moreover, the fitting analysis of carbon peaks evidences that the ratio between the polar peak components attributed respectively to single and double bonds of carbon to heteroatoms (including peptide linkages) are 2 : 1 on hydrophobic and 1 : 1 on hydrophilic surfaces after Lf immobilization (see ESI†).

This data interpretation is further supported by AFM imaging, which evidences the occurrence of different protein aggregation processes on the hydrophobic and hydrophilic polymer areas. Fig. 3 shows small Lf aggregates homogeneously distributed on the hydrophilic polymer surfaces (Fig. 3(d)), while larger and taller aggregates are observed on the hydrophobic areas (Fig. 3(b)). Moreover, the statistical analysis of grain sizes evidences a quite narrow distribution on the hydrophilic areas, centered at about 1.8 nm of height, while a wider distribution is found for the hydrophobic substrate, where the tallest maximum corresponds to about 4.8 nm.

It is of note that the high smoothness of untreated polymer is not affected by oxygen plasma treatment; both the substrates have roughness values below 0.5 nm (Fig. 3(a) and (c)).

The topography and corresponding section analysis graphs of HYL-np and HYB-np nanopatterned polymer surfaces, before and after the Lf immobilization, are shown in Fig. 4.

It is well evident that the opposite protein adsorption behavior is obtained for the hydrophilic and hydrophobic nanopore arrays. In fact, both pore depths and diameters decrease (or increase) for HYL-np (or HYB-np) after lactoferrin immobilization, indicating the preferential gathering of Lf molecules inside the hydrophilic or outside the hydrophobic domains, respectively.

The statistical analysis of AFM images for depth and diameter values is shown in Fig. 5.

It should be noted that the adsorbed amounts calculated by simple extrapolation of the mass values on the larger areas, as measured by QCM-D, do not correlate with the observed effect of preferential adsorption on the nanopores. On the other hand, the AFM results can be explained by an effect of

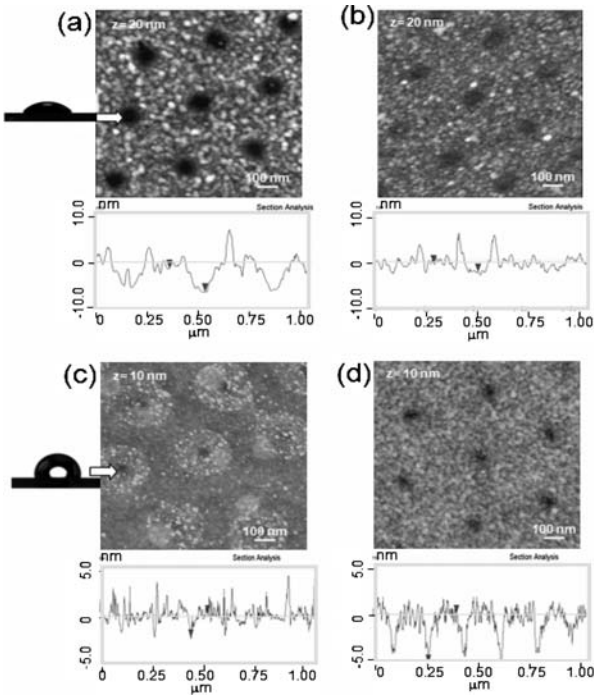

Fig. 4 AFM height images and corresponding section analysis curves for: (a) bare HYL-np, (b) Lf immobilized on HYL-np, (c) bare HYB-np, (d) Lf immobilized on HYB-np.

size confinement/exclusion of the Lf molecule aggregates into the nanopore arrays.

Indeed, the large protein aggregates observed on the hydrophobic polymer areas are likely not favoured to adsorb into the small hydrophobic areas of the nanostructured HYB-np substrates. On the contrary, the smaller protein aggregates observed onto the hydrophilic areas do not hinder the adsorption of lactoferrin molecules into the hydrophilic pores at the HYL-np surfaces.

Fig. 5(c) is a sketch of the pore surface chemistry profile and the confined protein aggregates immobilization effect.

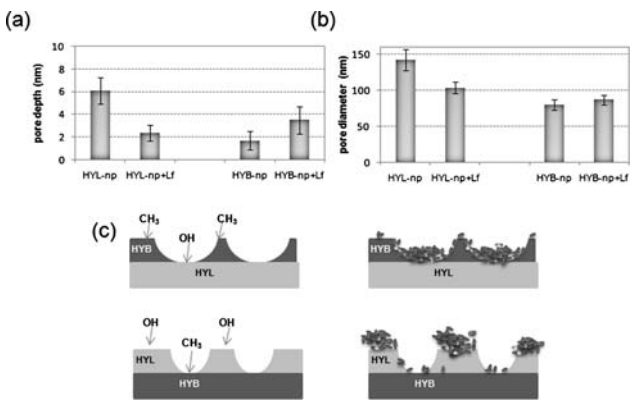

Fig. 5 Characteristics pore depths (a) and pore diameters (b) of HYL-np and HYB-np, before and after the Lf immobilization. (c) A cartoon representing the preferential adsorption of Lf molecules aggregates inside the nanopore area for HYL-np or outside the pore area for HYB-np.

A systematic study is currently in progress for the correlation between the topographical characteristics of the nanopore arrays (*i.e.*, pore depth, pore diameter, rim height), and the average dimensions of the protein aggregates.

In conclusion, we obtained preferential immobilization of lactoferrin inside or outside nanopores by spontaneous protein adsorption on nanostructured polymer surfaces consisting of two-dimensional hydrophilic/hydrophobic nanopore arrays.

It must be stressed that this approach allows adsorption of protein molecules into the nanopore arrays by non-covalent immobilization. Thus, it is very promising for potential applications of the nanopatterned polymer films, which can be easily deposited at the surface of suitable substrates, as nanocontainers in mass transport and release processes, *e.g.*, drug delivery, nanomedicine, *etc*. The confinement of the protein inside the dense nanopore arrays would offer the advantages of higher control of loading and release processes compared to traditional methods with homogeneous substrates or particles.

Further investigations are in progress to verify the activity of the immobilized protein molecules in the nanopore arrays, as well as to enhance the observed preferential adsorption behaviour to completely selective immobilization.

Notes and references

‡ The calculated amounts are 0.63 ± 0.02 μg cm^{-2} on hydrophobic and 0.76 ± 0.02 μg cm^{-2} on hydrophilic areas, respectively, which corresponds approximately to three monolayers of Lf molecules in end-on orientation or to 7–8 monolayers of Lf molecules in side-on orientation.

1 J. H. Moon, W. S. Kim, J.-W. Ha, S. G. Jang, S.-M. Yang and J.-K. Park, *Chem. Commun*., 2005, 4107.
2 L. S. McCarty, A. Winkleman and G. M. Whitesides, *Angew. Chem., Int. Ed*., 2007, **46**, 206.
3 X. Chen, Z. Chen, N. Fu, G. Lu and B. Yang, *Adv. Mater*., 2003, **15**, 1413.
4 L. Wang, M. H. Lee, J. Barton, L. Hughes and T. W. Odom, *J. Am. Chem. Soc*., 2008, **130**, 2142.
5 J. Yuan, L. Qu, D. Zhang and G. Shi, *Chem. Commun*., 2004, 994.
6 A. Sadana, *Chem. Rev*., 1992, **92**, 1799.
7 P. Cha, A. Krishnan, V. F. Fiore and E. A. Vogler, *Langmuir*, 2008, **24**, 2553.
8 J. Zimmermann, M. Rabe, D. Verdes and S. Seeger, *Langmuir*, 2008, **24**, 1053.
9 M. Schoen, *Phys. Chem. Chem. Phys*., 2008, **10**, 223.
10 R. Lipowsky, *Curr. Opin. Colloid Interface Sci*., 2001, **6**, 40.
11 S. Vaitheeswaran and D. Thirumalai, *J. Am. Chem. Soc*., 2006, **128**, 13490.
12 Y. Wang, S. Han, A. L. Briseno, R. J. G. Sanedrin and F. J. Zhou, *J. Mater. Chem*., 2004, **14**, 3488.
13 J.-R. Li, G. C. Henry and J. C. Garno, *Analyst*, 2006, **131**, 244.
14 C. Bae, H. Shin, J. Moon and M. M. Sung, *Chem. Mater*., 2006, **18**, 1085.
15 C. Satriano, G. Marletta and B. Kasemo, *Surf. Interface Anal*., 2008, **40**, 649.
16 R. García, R. Magerle and R. Perez, *Nat. Mater*., 2007, **6**, 405.
17 E. Reimhult, C. Larsson, B. Kasemo and F. Höök, *Anal. Chem*., 2004, **76**, 7211.
18 As estimated by considering the Lf molecular dimensions of 5.6 × 9.5 × 15.2 (nm^3) from J. R. Lu, S. Perumal, X. Zhao, F. Miano, V. Enea, R. R. Heenan and J. Penfold, *Langmuir*, 2005, **21**, 3354.
19 L.-C. Xu and C. A. Siedlecki, *Biomaterials*, 2007, **28**, 3273.
20 P. Roach, D. Farrar and C. C. Perry, *J. Am. Chem. Soc*., 2006, **128**, 3939.